Journal of the Iranian Chemical Society
https://doi.org/10.1007/s13738-017-1237-3

ORIGINAL PAPER

Heteropolyacid immobilized on polymer/magnetic zeolite nanocomposite as a new and recyclable catalyst for the selective oxidation of alcohols

Maryam Maleki[1] · **Seyed Meysam Baghbanian**[1] · **Mahmood Tajbakhsh**[2]

Received: 26 July 2016 / Accepted: 14 November 2017

Abstract
A new magnetic oxidation catalyst was prepared using immobilization of tungstophosphoric acid on poly(*N*-vinylimidazole) entrapped magnetic nanozeolite and characterized by FTIR, TGA, XRD, SEM, TEM, EDX, VSM, and ICP-OES. The resulting heterogeneous catalyst displays high catalytic performance for selective oxidation of alcohols compared to the other catalysts. The catalyst could be reused eight times without any loss of catalytic activity.

Keywords Magnetic nanozeolite · Poly(*N*-vinylimidazole) · Tungstophosphoric acid · Selective oxidation · Alcohols

Introduction

Oxidation reaction of different primary and secondary alcohols to carbonyl compounds is one of the critical reactions and key transformations at both laboratory and commercial scales [1]. The oxidation of alcohols using several kinds of reagents has already been investigated [2]. Among them, hydrogen peroxide as an inexpensive and commercially accessible reagent, is an significance oxidant due to it can be safely stored and employed and its low standard redox potential in some acidic media [2, 3]. Several metals such as manganese, rhenium, molybdenum, and ruthenium have been applied as homogeneous catalysts in oxidation reactions [4–63]. Among them, tungsten is the most considered to selective oxidation of alcohols due to its selectivity and efficiency in this reaction. As a result, several catalysts based on tungstate have been reported for oxidation of alcohols using H_2O_2 but most of them are homogeneous and have problems such as separation and recovery catalyst, lack of selectivity, and limit their use in industrial applications [64–68].

To solve these problems, an acceptable method is immobilization of tungsten as homogeneous catalyst on the organic (polymers [69–75]) and inorganic (silica [76–79], mesoporous silica [80–83], magnetic nanoparticles [72, 84, 85], and graphene oxide [86]) supports. Among inorganic supports, magnetic nanozeolite clinoptilolite (MNZ) is an attractive support because of the excellent properties such as inexpensive, good thermal and chemical stability, and easy separation without the need for any filtration or centrifugation processes [87–89, 92].

The supported ionic liquid technology is a fundamental, new method to achieve liquid, including solid materials that do not evaporate, made through surface modification of a porous solid [90]. In supported ionic liquid catalysis, the focus has been mainly on the immobilization homogeneous transition metals inside the thin ILs. The main drawback of homogeneous catalysis is the recovering of the dissolved catalyst from the reaction mixture that commonly can be by distillation or extraction. This problem has restricted the applications of homogeneous catalysts in multi-step reactions that can be circumvented by the supported ionic liquid technology [90].

In order to solve the above problems and introduce a new catalyst for the oxidation of alcohols, herein we wish to report a convenient method for selective oxidation of primary alcohols to their corresponding aldehydes with 12-tungstophosphoric acid immobilization onto poly(N-vinylimidazole)-modified magnetic nanozeolite (MNZ@PVImW) as a catalyst.

✉ Seyed Meysam Baghbanian
s.baghbanian@gmail.com; s.m.baghbanian@iauamol.ac.ir

[1] Department of Chemistry, Ayatollah Amoli Branch, Islamic Azad University, Amol, Iran

[2] Faculty of Chemistry, University of Mazandaran, Babolsar 47415, Iran

Experimental

Reagents and analysis

$FeCl_3{\cdot}6H_2O$, $FeCl_2{\cdot}4H_2O$, 3-methacryloxypropyltrimethoxy-silane (MPS, 98%), 1-bromododecane, 1-vinylimidazole, and ammonia (30%) were obtained from Aldrich. 1,4-dibromobutane and 2,2′-azobisisobutyronitrile (AIBN, 97%) were obtained from Merck. The raw zeolite material was an Iranian commercial clinoptilolite (CP) (Afrandtooska Company) obtained from deposits in the region of Semnan, Iran. The X-ray powder diffraction (XRD) of the catalyst was performed on a Philips PW 1800 X-ray diffractometer with a CuKα source (LEF tube, 40 kV, 50 mA). Thermogravimetric analyses (TGA) were taken under a nitrogen atmosphere using a PerkinElmer analyzer. Scanning electron microscope (SEM) picture was observed using a KYKY-EM 3200 microscope (acceleration voltage 26 kV). Energy dispersive spectroscopy (EDS) diagrams were recorded by a VEGA\\TESCAN-LMU scanning electron microscope. Transmission electron microscopy (TEM) experiments were conducted on a JEOL-2100 microscope operated at 200 kV. Fourier-transform infrared spectra of the samples were recorded on a Rayleigh WQF-510 FT-IR spectrometer using KBr disks. Magnetic measurements were performed using vibration sample magnetometer (VSM, MDK, and Model 7400, Kashan, Iran) analysis. Elemental analyses for C, H, and N were performed using a Heraeus CHN-O-Rapid analyzer. A simultaneous ICP-OES (Varian Vista-Pro, Springvale, Australia) coupled to a V-groove nebulizer and equipped with a charge-coupled device (CCD) was applied for determination of the trace metal ions. The composition of reaction mixture was analyzed by GC using an Agilent gas chromatograph fitted with a Factor Four HP-5MS capillary column.

General procedure

Synthesis of magnetic nanozeolite (MNZ)

For the synthesis of magnetite nanozeolite, first, 1 g of nanozeolite [91] was added to 50 mL of distilled water in a round bottom flask, ultra-sonicated for 15 min at room temperature, and deoxygenated by bubbling of N_2 gas for 30 min. After that, solutions of $FeCl_3$ (1 M in water) and $FeCl_2$ (2 M in HCl 2 M) with molar ratio of 4:1 (Fe^{3+}/Fe^{2+}) were added dropwise to the nanozeolite (NZ) mixture and stirred for 30 min [92]. Then, while the mixture was vigorously stirred, 70 mL of ammonia solution was slowly added into the mixture. When the color of solution changes from white to dark, the prepared composite was separated using a simple magnet, washed with distilled water several times, and finally dried in oven at 50°C for 6 h.

Synthesis of MPS-coated magnetic nanozeolite (MNZ@MPS)

Chemical modification of MNZ surface with MPS before polymerization causes grafting of polymer chains onto MNZ by covalent bonding. In other words, modification of MNZ by methacrylate groups causes polymerization easier on the surface of MNZ, and all of them are grafted by a copolymer shell [93]. As a result, MNZ (1 g) was dispersed in 15 mL of absolute ethanol, and then 2 mL of ammonium solution was added to the flask. After that, 10 mmol (excess) of the MPS solution was added slowly, and the mixture was stirred at 70 °C for 12 h. MNZ@MPS was magnetically separated and washed several times with ethanol and dried under vacuum at 65 °C.

Synthesis of 1,4-butanediyl-3,3′-bis-*L*-vinylimidazolium dibromide (BVD)

Typically, 1,4-butanediyl-3,3′-bis-*L*-vinylimidazolium dibromide (BVD) was synthesized based on a reported method [94]. 1-Vinylimidazole (2.82 g, 30 mmol) was dissolved in 15 mL ethanol, and 1,4-dibromobutane (3.24 g, 15 mmol) in 15 mL ethanol was added dropwise to the 1-vinylimidazole solution. The mixture was stirred at 60 °C for 10 h. After cooling of the reaction flask to ambient temperature, the reaction mixture was added dropwise into 500 mL of dry diethyl ether. The white powder was separated and dried at room temperature.

1,4-Butanediyl-3,3′-bis-*L*-vinylimidazolium dibromide (Mp = 148 °C). ^{1}H NMR (DMSO-d_6, δ, ppm): 9.55 (2H), 8.28 (2H), 7.93 (2H), 7.47 (2H), 5.92 (2H), 5.42 (2H), 4.30 (4H), 1.82 (4H). ^{13}C NMR (DMSO-d_6, δ, ppm): 134.9, 129.4, 123.8, 120.1, 109.2, 49.3, 26.4.

Synthesis of 12-tungstophosphoric acid immobilization onto poly(*N*-vinylimidazole) modified magnetic nanozeolite (MNZ@PVImW)

MNZ@MPS (0.5 g), 1-vinylimidazole (VIm) (1 mL), and BVD (0.3 g) were dissolved in methanol (50 mL) and ultrasonicated for 20 min at room temperature. Then, the mixture deoxygenated bubbling argon for another 20 min. Afterward, 0.008 g of AIBN was added into the mixture, and the flask was placed in an oil bath at 60 °C for 24 h. The precipitates (MNZ@PVIm) were magnetically separated from the solution, washed several times with methanol, and dried under vacuum at 50 °C. Next, the MNZ@PVIm (1 g) was dispersed in 50 mL deionized water with continuous ultrasonication and stirring for 30 min. Then, a solution of $H_3PW_{12}O_{40}$ 0.015 gr in 50 mL deionized water was added to the above mixture and stirred for 24 h at room temperature. The brown solid product (MNZ@PVImW) was magnetically separated, washed five times with deionized water (5 × 50 mL), twice with ethanol (2 × 25 mL), and dried under vacuum at 50 °C.

Catalytic oxidation of benzyl alcohols

In a typical procedure, benzyl alcohols (1 mmol), CH_3CN (3 mL), H_2O_2 (4 mmol), and MNP@PILW (2 mg) were added to a 50 mL round bottom flask. The reaction mixture was stirred at 40 °C for a defined time. After the reaction, the catalyst was separated from the mixture by a magnet. The product was extracted by ethyl acetate (5 mL) and then analyzed by gas chromatography (GC).

General procedure for oxidation of benzyl alcohols in large scale

A mixture of benzyl alcohols (10 mmol), CH_3CN (30 mL), H_2O_2 (40 mmol), and MNP@PILW (20 mg) was stirred at 40 °C for a defined time. After completion of reaction (monitored by TLC), the catalyst was magnetically separated, washed with CH_3CN, and dried for another run. The product was extracted by ethyl acetate (50 mL) and then analyzed by gas chromatography (GC).

Results and discussion

Production of the catalyst system

The MNZ was prepared by co-precipitation of $FeCl_3$ and $FeCl_2$ in the presence of natural nanozeolite. Next, the MPS was attached on the surface of MNZ by reaction of –OH groups on the MNZ and the $(MeO)_3$–Si groups in the MPS to form the active vinyl groups on the surface of MNZ. Afterward, MNZ entrapped cross-linked poly(*N*-vinylimidazole) was synthesized by copolymerization of 1-vinylimidazole (VIm) monomer in the presence of MNZ@MPS and BVD as cross-linked. Copolymerization begins by AIBN in methanol at 60 °C, and MNZ@PVIm copolymer was precipitated. In the next step, the generated copolymer was reacted with HPW to produce of MNZ@PVImW catalyst (Fig. 1).

Characterization of the catalyst

FT-IR spectra of (a) NZ, (b) MNZ, (c) MNZ@PVIm, and (d) MNZ@PVImW are shown in Fig. 2. In the spectrum of the NZ, the peak at 3853 and 3467 cm^{-1} corresponds to OH stretching of Si–OH and water, and the medium intensity band at 1637 cm^{-1} corresponds to the bending vibration of H–O–H groups. The strong band at 1095 cm^{-1} is related to the asymmetric stretching vibration of the Si–O and Al–O groups, and the weak bands at 476 cm^{-1} are due to bending vibrations of O–Si–O and O–Al–O groups [91]. The IR spectrum of MNZ revealed the changes in the framework configurations of zeolitic structure after the incorporation of Fe_3O_4. Changes occurred compared with NZ include the OH stretching vibrations at 3138 cm^{-1}, the Fe–O–Fe stretching vibrations at 598 cm^{-1}, and the weak stretching vibration of Fe–O at 476 cm^{-1}. The results show that Fe_3O_4 nanoparticles are formed into the NZ [89, 92, 95]. The spectrum of the MNZ@PVIm revealed the OH stretching vibrations at 3425 cm^{-1} and the C–H stretching vibrations of alkyl chains at 2925 cm^{-1}. Additionally,

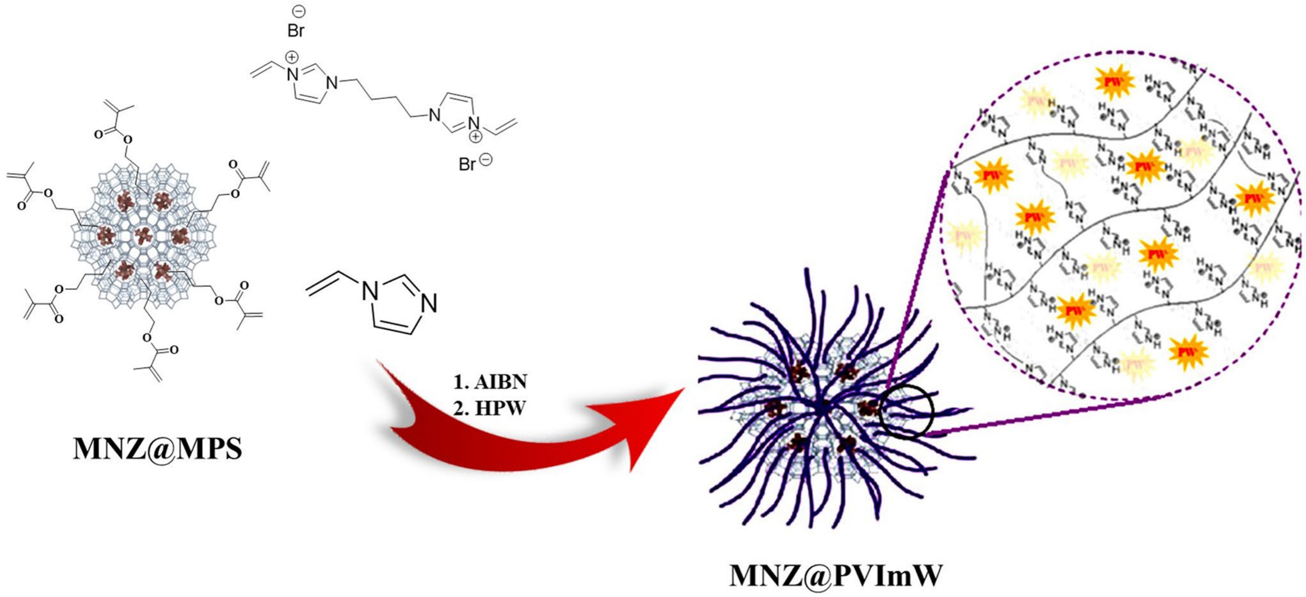

Fig. 1 Preparation of MNZ@PVImW

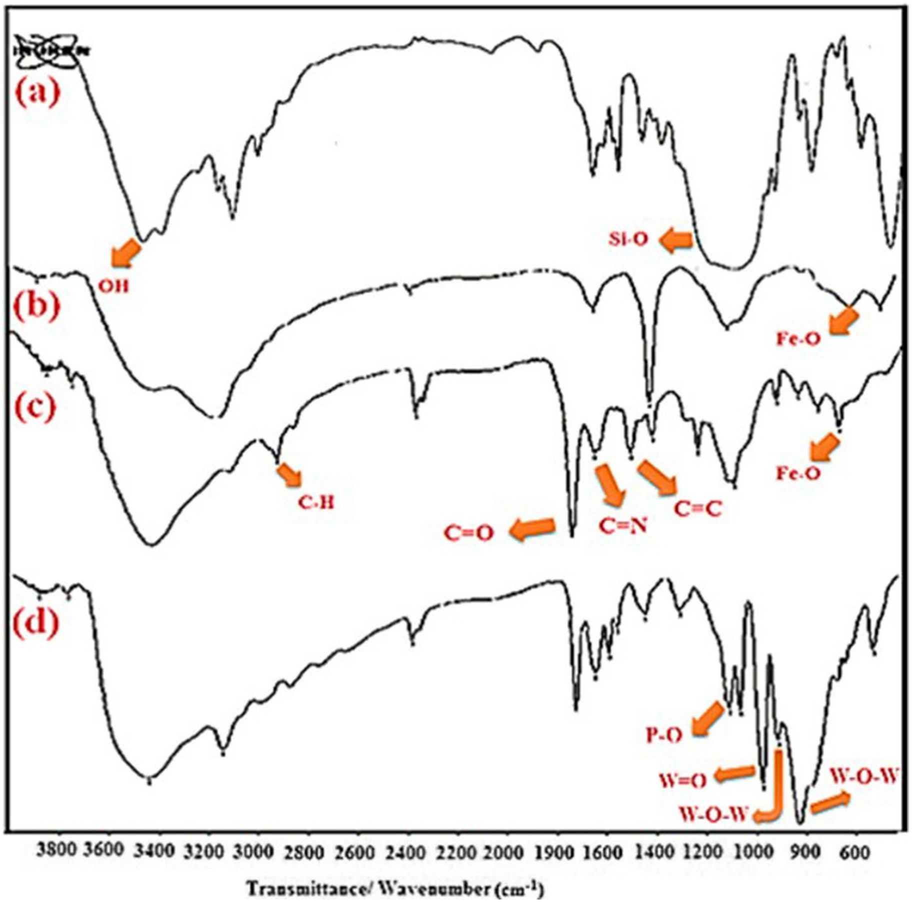

Fig. 2 FT-IR spectra (a) NZ, (b) MNZ, (c) MNZ@PVIm and (d) MNZ@PVImW

MNZ@PVIm shows stretching vibration of a carbonyl group at 1712 cm^{-1} and the C=N and C=C stretching vibrations of the imidazole ring at 1647 and 1501 cm^{-1}, respectively, that prove successful presence of PVIm on MNZ. For the spectrum of MNZ@PVImW, new peaks were observed at 805 and 895 cm^{-1} (W–O–W), 954 cm^{-1} (W=O), and 1091 cm^{-1} (P–O) that can be related to $[PW_{12}O_{40}]^{3-}$ anion [96, 97]. All the results achieved from FT-IR spectra approve that MNZ entrapped into the copolymers and the $[PW_{12}O_{40}]^{3-}$ ions were successfully entrapped into the polymeric matrix.

The thermal gravimetric analysis (TGA) of MNZ and MNZ@PVImW are exhibited in Fig. 3. In TGA curves of MNZ and MNZ@PVImW, a mass loss observed between room temperature and 200 °C could be related to the removal of surface adsorbed water. In the case of MNZ@PVImW, the second step weight loss (41%) starting from 250 °C to 600 °C was likely due to the thermal decomposition of the copolymer.

Patterns of XRD for NZ, MNZ, and MNZ@PVImW are investigated in Fig. 4. As shown in Fig. 4a, the obtained XRD pattern exhibited reflection peaks of NZ at 2θ = 21.74°, 27.46° and 35.92° found and identified as natural zeolite of clinoptilolite when compared with the standard pattern (green stars) (JCPDS 00-025-1349). The XRD patterns of MNZ (Fig. 4b) have the same characteristic peaks of zeolite with additional broad peaks at $2\theta = 35.81°$, 57.18°, and 62.74° related to the 311, 511, and 440 crystallographic planes of the face-centered cubic (FCC) iron oxide nanocrystals which fully comply with the standard Fe_3O_4 (orange balls) (JCPDS 19-0629) [98]. Figure 4c shows the XRD pattern of MNZ@PVImW with a broad peak, and low reflection intensity at 8–10°, 17–22°, and 24–40° can be assigned to the diffraction characteristic peaks of crystalline $H_3PW_{12}O_{40}$ Keggin structure [99].

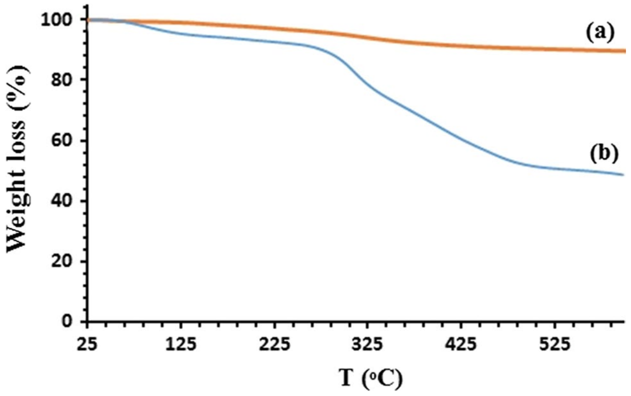

Fig. 3 TGA curves of (a) MNZ and (b) MNZ@PVImW

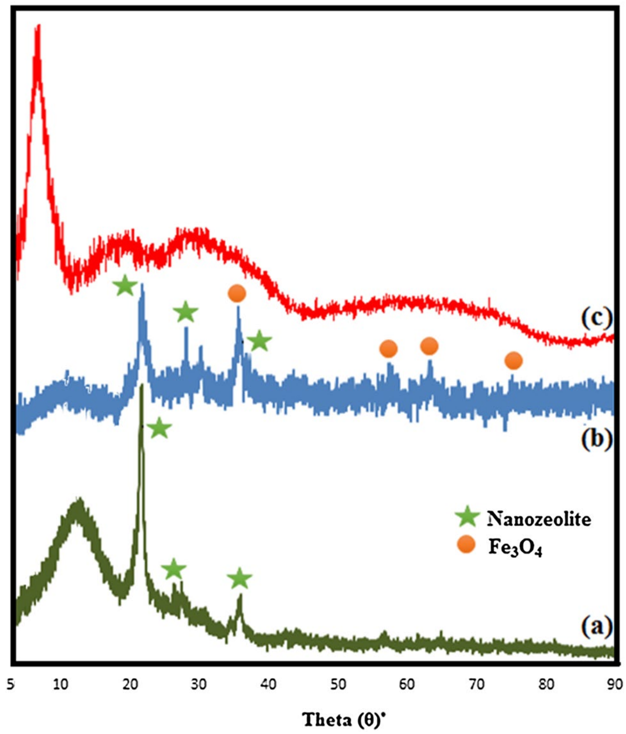

Fig. 4 XRD patterns of (a) NZ, (b) MNZ, and (c) MNZ@PVImW

The surface morphology of MNZ@PVImW was studied by SEM image (Fig. 5a). As can be seen, all the particles have similar structures. TEM image of MNZ@PVImW shows (Fig. 5b) that MNZ dispersed into the polymeric matrix and the $[PW_{12}O_{40}]^{3-}$ ions was entrapped into the copolymer. EDX analysis from the obtained MNZ@PVImW (Fig. 5c) showed the presence of the expected elements in the structure of the catalyst, namely oxygen (27.68%), iron (42.54%), aluminum (3.34%), silicon (16.83%), phosphorus (0.67%), and tungsten (8.49%).

Figure 6 shows the magnetization of MNZ and MNZ@PVImW at room temperature (300 K). The MNZ and MNZ@PILW showed an "*S*"-shaped hysteresis loop without remanence which indicates the particles have good superparamagnetic properties. The saturation magnetization of MNZ and MNZ@PILW was 47.7 and 27.6 emu/g, respectively. These results show that the magnetization of MNZ@PVImW decreased considerably with the formation copolymer on MNZ. However, the typical superparamagnetic behavior of MNZ@PVImW implies that the catalyst can be magnetically separated.

The total loading amount of tungstate ions in MNZ@PVImW was calculated by ICP-OES to be 9 wt% (0.04 mmol/g).

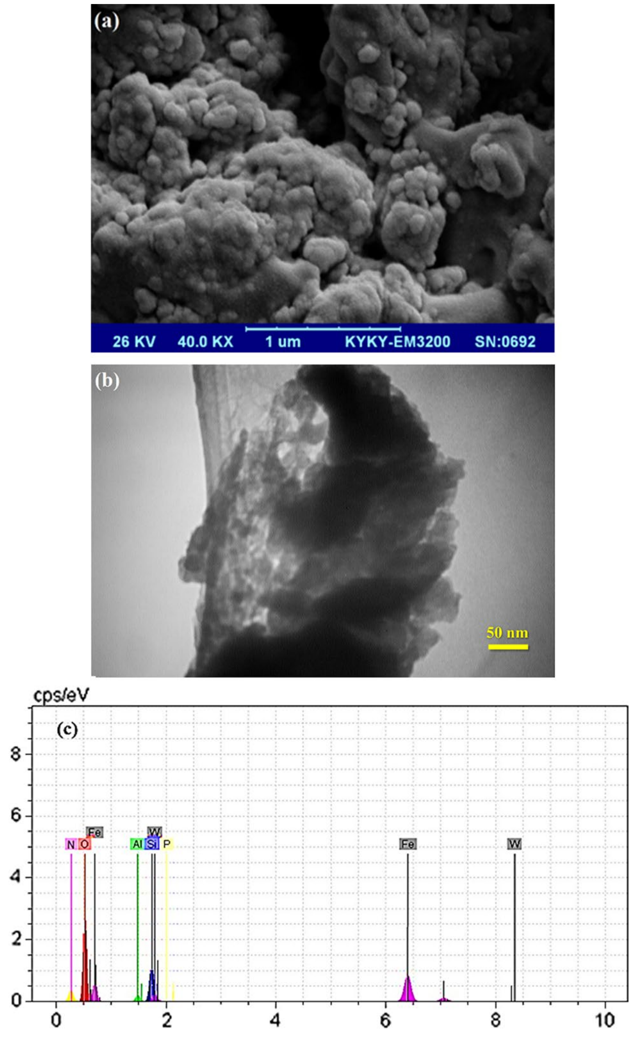

Fig. 5 **a** SEM, **b** TEM images, and **c** EDX analysis of MNZ@PVImW

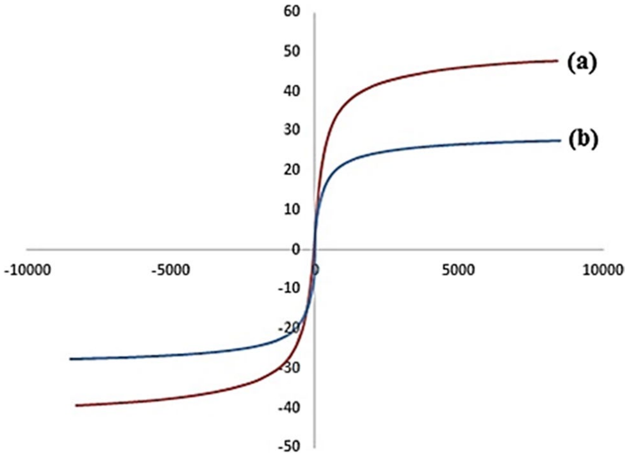

Fig. 6 Magnetization of (a) MNZ and (b)MNZ@PILW

Table 1 Results of oxidation of benzyl alcohol to benzaldehyde over various conditions

Entry	Catalyst	Amount of catalyst (mg)	Solvent	*T* (°C)	Time (min)	Conv.[a] (%)	Yield[b] (%)	Selectivity (%)	
								A	B
1	–	–	CH_3CN	40	60	–	–	–	–
2	MNZ@PVImW	1	CH_3CN	40	60	78	75	85.7	14.3
3	MNZ@PVImW	2	CH_3CN	40	30	96	95	95.4	4.6
4	MNZ@PVImW	4	CH_3CN	40	30	45	43	97.3	2.7
5	MNZ@PVImW	2	CH_3CN	r.t	30	64	60	78.2	21.8
6	MNZ@PVImW	2	CH_3CN	80	30	95	92	1.3	98.7
7[c]	MNZ@PVImW	2	CH_3CN	40	120	39	45	88.5	11.5
8	MNZ@PVImW	2	Water	40	30	75	78	80.9	19.1
9	MNZ@PVImW	2	Water	80	30	85	80	30.7	69.3
10	MNZ@PVImW	2	CH_2Cl2	r.t	60	25	28	89.3	10.7
11	MNZ@PVImW	2	CH_2Cl2	40	60	58	65	21.5	78.5
12	MNZ@PVImW	2	–	40	60	75	80	92.4	7.8
13	MNZ@PVImW	2	–	80	60	85	87	34.8	65.2
14	HPW	50	CH_3CN	40	120	68	65	64.6	35.4

Reaction conditions: benzyl alcohol (1 mmol), H_2O_2 (4 mmol), 3 mL solvent

[a] Conversions were calculated based on initial mmol of benzyl alcohol

[b] Yields were determined by GC

[c] 2 mmol H_2O_2

Catalyst activity study of MNZ@PVImW

Initially, in order to investigate the catalytic activity of MNZ@PVImW, the oxidation of benzyl alcohol to benzaldehyde was examined under different conditions as a model reaction, and the results were listed in Table 1. For the initial study, we used CH_3CN (3 mL) as solvent and H_2O_2 (4 mL) as oxidant for the oxidation of benzyl alcohol in the presence of MNZ@PVImW as catalyst at 40 °C. In the absence of catalyst, no desired product was formed (Table 1, entry 1). Oxidation of benzyl alcohol has been carried out over 1, 2, and 4 mg of catalyst under model reaction (Table 1, entries 2–4). The results revealed that both the conversion of benzyl alcohol and the selectivity of benzaldehyde increased. No obvious improvement was observed in the catalytic performance of MNZ@PVImW when catalyst loading increased to 4 g (Table 1, entry 4), but the selectivity increased from 95.4 to 97.3%. From the viewpoint of yield of benzaldehyde, 2 mg MNZ@PVImW gives the best results. (Table 1, entry 3). Oxidation of benzyl alcohol to benzaldehyde with H_2O_2 on MNZ@PVImW was explored in various temperatures (Table 1, entries 5 and 6). When the reaction was carried out at a higher temperature, the selectivity for benzaldehyde (A) was reduced with the formation of benzoic acid (B) from 95.4 to 1.3% at 80 °C (Table 1, entry 6). Also, the selectivity was decreased from 95.4 to 78.2% with reducing the temperature to 25 °C (Table 1, entry 5). According to the results, 40 °C was chosen to be the best reaction temperature for the selective oxidation of benzyl alcohol. To optimize the amount of H_2O_2, the oxidation of benzyl alcohol with 2 mmol H_2O_2 under same reaction conditions was investigated that demonstrated only 39% conversion is achieved in 2 h (Table 1, entry 7). Consequently, 4 mmol H_2O_2 is the optimum amount under these conditions. In order to optimize the reaction conditions, the model reaction was examined in various solvents such as H_2O and CH_2Cl_2 instead of CH_3CN, and results showed that CH_3CN is the best solvent for this reaction (Table 1, entries 8–11). The oxidation of benzyl alcohol was also investigated in solvent-free condition (Table 1, entries 12–14), the selectivity and yield of benzaldehyde were 92.4% and 80%, respectively. All these results demonstrate that the optimum conditions for oxidation reaction of benzyl alcohol to benzaldehyde is 2 mg MNZ@PVImW as catalyst and 4 mmol H_2O_2 in CH_3CN at 40 °C (Table 1, entry 3).

The MNZ@PVImW was evaluated in the catalytic oxidation of benzylic alcohols under optimized reaction conditions. The oxidations of various benzylic alcohols with electron-donating and electron-withdrawing substituents to corresponding aldehydes have been studied. Under this method, oxidation of substituted benzyl alcohols with electron-donor groups (CH_3, OCH_3) take place faster than benzylic alcohols with electron-withdrawing groups (Cl, NO_2). The reaction of cyclic alcohols such as cyclohexanol and aliphatic alcohols were also investigated, and results demonstrated that the desired products were obtained in lower yields and longer reaction times than benzylic alcohols.

Table 2 Oxidation of various alcohols catalyzed by MNZ@PVImW

Entry	Substrates	Product		Time (min)	Conv.^{a} (%)	Yield (%)
		A	B			
1	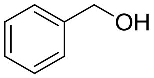	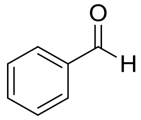	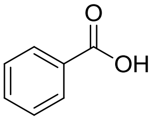	30	96	95
2	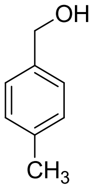	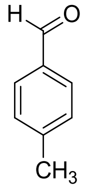	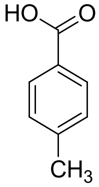	25	92	92
3	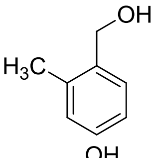	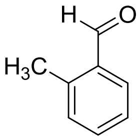	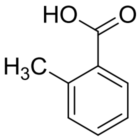	25	91	90
4	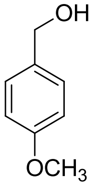	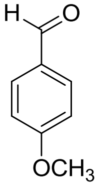	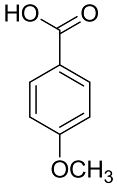	25	96	95
5	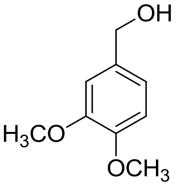	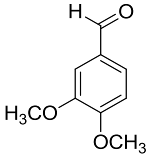	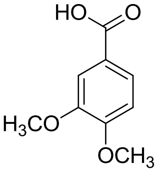	20	91	90
6	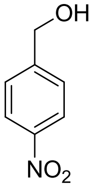	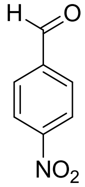	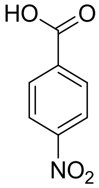	60	82	80
7	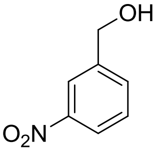	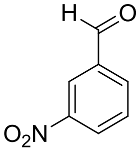	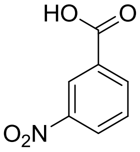	90	79	75
8	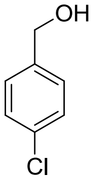	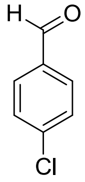	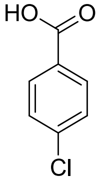	45	92	91
9	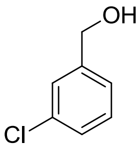	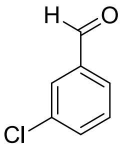	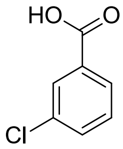	45	92	90

Table 2 (continued)

Entry	Substrates	Product A	Product B	Time (min)	Conv.[a] (%)	Yield (%)
10	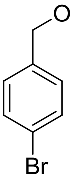	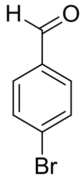	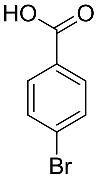	40	92	91
11	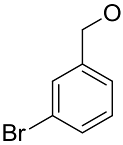	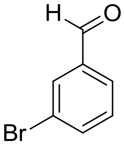	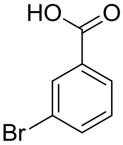	40	90	89
12	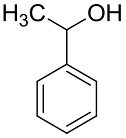	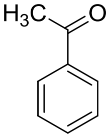	–	30	90	88
13	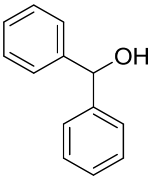	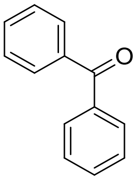	–	45	92	90
14	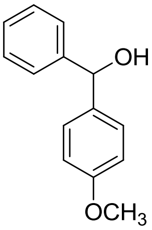	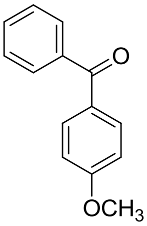	–	40	91	90
15	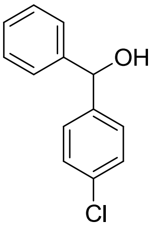	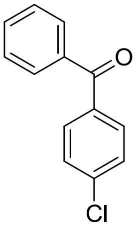	–	40	88	85
16	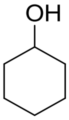	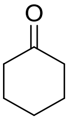	–	60	90	89
17	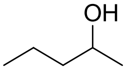	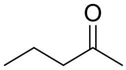	–	60	70	69
18	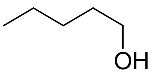	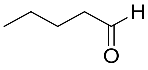	–	60	30	86

Reaction conditions: substrate (1 mmol), H_2O_2 (4 mmol), MNZ@PVImW (2 mg), CH_3CN (3 mL) and 40 °C

[a] Conversions were calculated based on initial mmol of benzyl alcohol

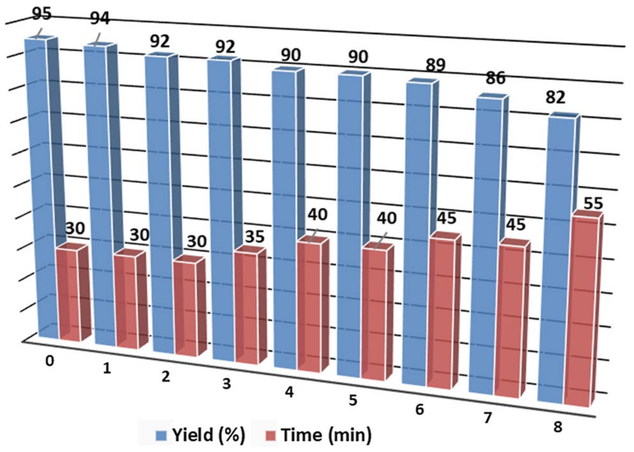

Fig. 7 Reusability of MNZ@PVImW in selective oxidation of benzyl alcohol to the benzaldehyde

Therefore, chemoselectivity with this catalyst was observed (Table 2).

In order to examine the recyclability of MNZ@PVImW in a large scale, we examined the reaction in the scale of 10 mmol. In this regard, after each run, the catalyst was separated by an external magnet and reused as such for the next experiment. As seen in Fig. 7, the efficiency of this catalyst remained unchanged even after eight runs. Although the catalyst can be easily separated by magnets from the reaction mixture, such studies are not enough to prove tungsten leaching from the polymer matrix. Therefore, in other methods, tungsten leaching from the magnetic support was investigated in the oxidation of benzyl alcohol. The model reaction was stopped after 15 min and the catalyst was removed from the solution and the yield was calculated by GC. Then, the reaction mixture was allowed to stir for another 15 min without catalyst, and the results show that no benzaldehyde is generated in the absence of catalyst. After separation of the catalyst, tungsten leaching into the reaction mixture was also detected with AAS and indicated that no tungsten has leached out from the polymer support.

Conclusion

In conclusion, in this work for the first time, a novel magnetic natural nanozeolite catalyst based on poly(*N*-vinylimidazole) was prepared and applied for selective oxidation of various alcohols. The catalyst could be easily separated using an external magnet and reused for several times without any significant loss of its activity. From the viewpoint of green chemistry, the used support is natural and accessible in underground mines that can be easily converted at least cost to the magnetic nanocomposite. Thus, this catalyst will be able to be used on a large scale.

Acknowledgements This research is supported by the Islamic Azad University, Ayatollah Amoli Branch, I. R. Iran.

References

1. B.S. Lane, K. Burgess, Chem. Rev. **103**, 2457–2473 (2003)
2. F. Shirini, M. Abedini, S.V. Atghia, in Green Solvents II, Properties and Applications of Ionic Liquids, ed. by A. Mohammad, D. Inamuddin (Springer, Chapter 14, Berlin), pp. 363–398 (2012)
3. W. Ando, in *In the Chemistry of Peroxides*, vol. 2, ed. by Z. Rappoport (Wiley, Chinchester, 2007), p. 778
4. P. Sharma, A. Lazar, A.P. Singh, Appl. Catal. A **439–440**, 101–110 (2012)
5. P. Zhao, M. Zhang, Y. Wu, J. Wang, Ind. Eng. Chem. Res. **6641**, 6647 (2012)
6. K. Yamaguchi, K. Mori, T. Mizugaki, K. Ebitani, K. Kaneda, J. Am. Chem. Soc. **122**, 7144–7145 (2000)
7. K. Yamaguchi, N. Mizuno, Angew. Chem. Int. Ed. **41**, 4538–4542 (2002)
8. K. Ebitani, K. Motokura, T. Mizugaki, K. Kaneda, Angew. Chem. Int. Ed. **44**, 3423–3426 (2005)
9. M. Kotani, T. Koike, K. Yamaguchi, N. Mizuno, Green Chem. **8**, 735–741 (2006)
10. K. Mori, S. Kanai, T. Hara, T. Mizugaki, K. Ebitani, K. Jitsukawa, K. Kaneda, Chem. Mater. **19**, 1249–1256 (2007)
11. C. Mondelli, D. Ferri, A. Baiker, J. Catal. **258**, 170–176 (2008)
12. S. Mori, M. Takubo, K. Makida, T. Yanase, S. Aoyagi, T. Maegawa, Y. Monguchi, H. Sajiki, Chem. Commun. **34**, 5159–5161 (2009)
13. K. Mori, K. Yamaguchi, T. Hara, T. Mizugaki, K. Ebitani, K. Kaneda, J. Am. Chem. Soc. **124**, 11572–11573 (2002)
14. D.R. Jensen, M.J. Schultz, J.A. Mueller, M.S. Sigman, Angew. Chem. Int. Ed. **42**, 3810–3813 (2003)
15. K. Mori, T. Hara, T. Mizugaki, K. Ebitani, K. Kaneda, J. Am. Chem. Soc. **126**, 10657–10666 (2004)
16. U.R. Pillai, E. Sahle-Demessie, Green Chem. **6**, 161–165 (2004)
17. M.S. Kwon, N. Kim, C.M. Park, J.S. Lee, K.Y. Kang, J. Park, Org. Lett. **7**, 1077–1079 (2005)
18. B. Karimi, Z. Zamani, J.H. Clark, Organometallics **24**, 4695–4698 (2005)
19. K. Karimi, S. Abedi, J.H. Clark, V. Budarin, Angew. Chem. Int. Ed. **45**, 4776–4779 (2006)
20. K. Hara, S. Tayama, H. Kano, T. Masuda, S. Takakusagi, T. Kondo, K. Uosaki, M. Sawamura, Chem. Commun. **41**, 4280–4282 (2007)
21. A.H. Lu, W.C. Li, Z. Hou, F. Schüth, Chem. Commun. **10**, 1038–1040 (2007)
22. S.F.J. Hackett, R.M. Brydson, M.H. Gass, I. Harvey, A.D. Newman, K. Wilson, A.F. Lee, Angew. Chem. Int. Ed. **46**, 8593–8596 (2007)
23. E.V. Chubarova, M.H. Dickman, B. Keita, L. Nadjo, F. Miserque, M. Mifsud, I.W.C.E. Arends, U. Kortz, Angew. Chem. Int. Ed. **47**, 9542–9546 (2008)
24. Z. Hou, N. Theyssen, A. Bronkmann, K.V. Klementiev, W. Grünert, M. Bühl, W. Schmidt, B. Spliethoff, B. Tesche, C. Weidenthaler, W. Leitner, J. Catal. **258**, 315–323 (2008)
25. S. Samanta, A.K. Nandi, J. Phys. Chem. C **113**, 4721–4725 (2009)
26. B. Karimi, A. Zamani, S. Abedi, J.H. Clark, Green Chem. **11**, 109–119 (2009)
27. T. Hara, M. Ishikawa, J. Sawada, N. Ichikuni, S. Shimazu, Green Chem. **11**, 2034–2040 (2009)
28. V. Polshettiwar, R.S. Varma, Org. Biomol. Chem. **7**, 37–40 (2009)
29. D. Barats, R. Neumann, Adv. Synth. Catal. **352**, 293–352 (2010)
30. N. Banda, P.Das Aggarwal, Tetrahedron Lett. **52**, 4954–4956 (2011)
31. C.M.A. Parlett, D.W. Bruce, N.S. Hondow, M.A. Newton, A.F. Lee, K. Wilson, ChemCatChem **5**, 939–950 (2013)

32. E.V. Johnston, O. Verho, M.D. Karkas, M. Shakeri, C.W. Tai, P. Palmgren, K. Eriksson, S. Oscarsson, J.E. Backvall, Chem. Eur. J. **18**, 12202–12206 (2012)
33. B. Karimi, H. Behzadnia, M. Bostina, H. Vali, Chem. Eur. J. **18**, 8634–8640 (2012)
34. V. Ravat, I. Nongwe, R. Meijboom, G. Bepete, N. Coville, J. Catal. **305**, 36–45 (2013)
35. B. Karimi, M. Khorasani, H. Vali, C. Vargas, R. Luque, ACS Catal. **5**, 4189–4200 (2015)
36. Y.M.A. Yamada, T. Arakawa, H. Hocke, Y. Uozumi, Angew. Chem. Int. Ed. **46**, 704–706 (2007)
37. T. Wang, C.X. Xiao, L. Yan, L. Xu, J. Luo, H. Shou, Y. Kou, H. Liu, Chem. Commun. **12**, 4375–4377 (2007)
38. C. Miyamura, R. Matsubara, S. Kobayashi, Chem. Commun. **17**, 2031–2033 (2008)
39. Y.H. Ng, S. Ikeda, Y. Morita, T. Harada, K. Ikeue, M. Matsumura, J. Phys. Chem. C **112**, 12799–12805 (2009)
40. A. Abad, C. Concepcion, A. Corma, H. Garcia, Angew. Chem. Int. Ed. **44**, 4066–4069 (2005)
41. F.Z. Su, Y.M. Liu, L.C. Wang, Y. Cao, H.Y. He, K.N. Fan, Angew. Chem. Int. Ed. **47**, 334–337 (2008)
42. T. Mitsudome, A. Noujima, T. Mizugaki, K. Jitsukawa, K. Kaneda, Adv. Synth. Catal. **351**, 1890–1896 (2009)
43. C. Lucchesi, T. Inasaki, H. Miyamura, R. Matsubara, S. Kobayashi, Adv. Synth. Catal. **350**, 1996–2000 (2008)
44. X. Wang, H. Kawanami, N.M. Islam, M. Chattergee, T. Yokoyama, T. Ikushima, Chem. Commun. **37**, 4442–4444 (2008)
45. H. Miyamura, R. Matsubara, Y. Miyazaki, S. Kobayashi, Angew. Chem. Int. Ed. **46**, 4151–4154 (2007)
46. B. Karimi, F.Esfahani Kabiri, Chem. Commun. **37**, 5555–5557 (2009)
47. H. Tsunoyama, H. Sakurai, Y. Negishi, T. Tsukuda, J. Am. Chem. Soc. **127**, 9374–9375 (2005)
48. S. Kanaoka, N. Yagi, Y. Fukuyama, S. Aoshima, H. Tsunoyama, T. Tsukuda, H. Sakurai, J. Am. Chem. Soc. **129**, 12060–12061 (2007)
49. S. Kim, S.W. Bae, J.S. Lee, J. Park, Tetrahedron **65**, 1461–1466 (2009)
50. K. Kaizuka, H. Miyamura, S. Kobayashi, J. Am. Chem. Soc. **132**, 15096–15098 (2010)
51. I.E. Marko, P.R. Giles, M. Tsukazaki, S.M. Brown, C.J. Urch, Science **274**, 2044–2046 (1996)
52. P. Gamez, I.W.C.E. Arends, J. Reedijka, R.A. Sheldon, Chem. Commun. **19**, 2414–2415 (2003)
53. N. Jiang, A.J. Ragauskas, Chemsuschem **1**, 823–825 (2008)
54. L. Lina, M. Juanjuana, J. Liuyana, W. Yunyang, J. Mol. Catal. A Chem. **291**, 1–4 (2008)
55. A. Kumar, Catal. Commun. **8**, 913–916 (2007)
56. P. Jin, Z. Zhao, Z. Dai, D. Wei, M. Tang, X. Wang, Catal. Today **175**, 619–624 (2011)
57. B. Karimi, F. Bakhshandeh Rostami, M. Khorasani, D. Elhamifar, H. Vali, Tetrahedron **70**, 6114–6119 (2014)
58. Y. Chen, R. Tan, W. Zheng, Y. Zhang, G. Zhao, D. Yin, Catal. Sci. Technol. **4**, 4084–4092 (2014)
59. Y. Zhou, G. Chen, Z. Long, J. Wang, RSC Adv. **4**, 42092–42113 (2014)
60. E. Skliri, I.N. Lykakis, G.S. Armatas, RSC Adv. **4**, 46170–46178 (2014)
61. B. Ma, W. Zhao, F. Zhang, Y. Zhang, S. Wu, Y. Ding, RSC Adv. **4**, 32054–32062 (2014)
62. W. Zhao, Y. Zhang, B. Ma, Y. Ding, W. Qiu, Catal. Commun. **11**, 527–531 (2010)
63. A. Pourjavadi, S.H. Hosseini, F.M. Moghaddam, B. Koushki Foroushani, C. Bennett, Green Chem. **15**, 2913–2919 (2013)
64. Z. Xi, N. Zhou, Y. Sun, K. Li, Science **292**, 1139–1141 (2001)
65. A. Haimov, H. Cohen, R. Neumann, J. Am. Chem. Soc. **126**, 11762–11763 (2014)
66. H. Hamamoto, Y. Suzuki, H. Takahashi, S. Ikegami, Tetrahedron Lett. **48**, 4239–4242 (2007)
67. G.D. Yadav, C.K. Mistry, J. Mol. Catal. A: Chem. **172**, 135–149 (2001)
68. M. Hulce, D.W. Marks, J. Chem. Educ. **78**, 66–70 (2001)
69. Y. Huang, W. Wang, Q. Feng, F. Dong, J. Saudi Chem. Soc. **21**, 58–66 (2017)
70. V. Javanbakht, S.M. Ghoreishi, N. Habibi, M. Javanbakht, Powder Technol. **302**, 372–383 (2016)
71. W. Wang, Q. Feng, K. Liu, G. Zhang, J. Liu, J. Huang, Solid State Sci. **39**, 52–58 (2015)
72. J. Zhu, P.C. Wang, M. Lu, New J. Chem. **36**, 2587–2592 (2012)
73. Y. Leng, J. Liu, P. Jiang, J. Wang, RSC Adv. **2**, 11653–11656 (2012)
74. Y. Leng, W. Zhang, J. Wang, P. Jiang, Appl. Catal. A **445–446**, 306–311 (2012)
75. Y. Leng, J. Wang, P. Jiang, Catal. Commun. **27**, 101–104 (2012)
76. X. Shi, J. Wei, J. Mol. Catal. A Chem. **280**, 142–147 (2008)
77. K. Yamaguchi, C. Yoshida, S. Uchida, N. Mizuno, J. Am. Chem. Soc. **127**, 530–531 (2005)
78. B. Karimi, M. Ghoreishi-Nezhad, J.H. Clark, Org. Lett. **7**, 625–628 (2005)
79. M. Vafaeezadeh, M.M. Hashemi, M. Shakourian-Fard, Catal. Commun. **26**, 54–57 (2012)
80. X. Yanga, W. Daia, H. Chena, J. Xua, Y. Caoa, H. Lib, K. Fan, Appl. Catal. A **283**, 1–8 (2005)
81. R. Zhang, W. Ding, B. Tu, D. Zhao, Chem. Mater. **19**, 4379–4381 (2007)
82. X. Yanga, W. Daia, R. Gaoa, H. Chena, H. Lib, Y. Caoa, K. Fan, J. Mol. Catal. A Chem. **241**, 205–214 (2005)
83. C. Chenga, K. Lina, M.R. Prasada, S. Fua, S. Changa, S. Shyub, H. Sheuc, C. Chenc, C. Chuangd, M. Lin, Catal. Commun. **8**, 1060–1064 (2007)
84. X. Xua, X. Shena, G. Zhua, L. Jinga, X. Liua, K. Chen, Chem. Eng. J. **521–531**, 200–202 (2012)
85. A. Konga, P. Wang, H. Zhang, F. Yang, S. Huang, Y. Shan, Appl. Catal. A **417–418**, 183–189 (2012)
86. K. Liu, T. Chen, Z. Hou, Y. Wang, L. Dai, Catal. Lett. **144**, 314–319 (2014)
87. N. Arabpour, A. Nezamzadeh-Ejhieh, Mater. Sci. Semicond. Process. **31**, 684–692 (2015)
88. W.Q. Wang, Q.M. Feng, F.Q. Dong, X.D. Zhao, J. Inorg. Mater. **25**, 401–405 (2010)
89. A. Mollahosseini, M. Toghroli, J. Asian Sci. Res. **5**, 120–125 (2015)
90. P.W.N.M. Leeuwen (ed.), *Homogeneous Catalysis* (Springer, Dordrecht, 2005)
91. S.M. Baghbanian, N. Rezaei, H. Tashakkorian, Green Chem. **15**, 3446–3458 (2013)
92. H. Faghihian, M. Moayed, A. Firooz, M. Iravani, C. R. Chim. **17**, 108–117 (2014)
93. W. Ma, S. Xu, J. Li, J. Guo, Y. Lin, C. Wang, J. Polym. Sci. Polym. Chem. **43**, 2725 (2011)
94. J. Yuan, M. Antonietti, Macromolecules **44**, 744–750 (2011)
95. J.L. Cao, X.W. Liu, R. Fu, Z. Tan, Sep. Purif. Technol. **63**, 92–100 (2008)
96. D. Chen, A. Sahasrabudhe, P. Wang, A. Dasgupta, R. Yuan, S. Roy, Dalton Trans. **42**, 10587–10596 (2013)
97. C. Pichon, P. Mialane, J. Marrot, C. Binet, A. Vimont, A. Travert, J.C. Lavalley, Phys. Chem. Chem. Phys. **13**, 322–327 (2011)
98. S. Hosseini, H. Jahangirian, M.H. Shahismail, M.J. Haron, R. Moghaddam, K. Shameli, K. Kalantari, R. Khandanlou, E. Gharibshahi, S. Soltaninejad, Dig. J Nanomater. Biostruct. **8**, 1405–1413 (2013)
99. E.B. Wang, C.W. Hu, L. Xu, *Polyhydric Chemistry Introduction* (Chemical Industry Press, Beijing, 1998)